Far-infrared nonlinear optics. I. $\chi^{(2)}$ near ionic resonance

A. Mayer* and F. Keilmann
Max-Planck-Institut für Festkörperforschung, 7000 Stuttgart 80, Federal Republic of Germany
(Received 12 November 1985)

Frequency doubling is used to determine absolutely $\chi^{(2)}(2\omega,\omega,\omega)$ of GaAs and $LiTaO_3$ at far-infrared frequencies, $20 \leq \omega \leq 57$ cm^{-1}. Resonant enhancement is observed in $LiTaO_3$ as an ionic resonance is approached. The technique employed in this study is extendable to the 200-cm^{-1} range, where it appears feasible to experimentally distinguish between mixed electronic-ionic contributions such as the third-order lattice potential and second-order dipole moment.

I. INTRODUCTION

Since the availability of lasers, a very large body of nonlinear optical work at visible and near-infrared frequencies has accumulated. It was spurred by such practical applications as frequency conversion or phase conjugation. High efficiency is readily observed.

In contrast, no bulk nonlinearities have been measured in the far-infrared spectral region until now. Here, much smaller efficiencies are expected because of strongly frequency-dependent phase space factors proportional to ω^n, where $n \geq 2$.

At still lower microwave frequencies, nonlinear optic coefficients are available from the work of Boyd *et al.*[1] In this region, use can be made of sensitive waveguide techniques such as filtering, modulation, and coherent detection. However, additional microwave work has not appeared, since, from the applications point of view, any low-power frequency conversion can efficiently be done with lumped elements (such as diodes, which make use of capacitive field concentration). Furthermore, the availability of high-power electron tubes throughout the microwave range does not necessitate high-power bulk frequency conversion.

From a fundamental point of view, there is an interesting distinction between optical and low-frequency nonlinear response.[1] As is well known, the dielectric function at optical frequencies is given solely by electronic response, while at sufficiently low frequency, *ionic motions* contribute. In crystals, the critical frequency is the lattice dipole or reststrahlen resonance, typically situated in the middle infrared, $100 \lesssim \omega \lesssim 500$ cm^{-1}. Therefore, nonlinear dielectric coefficients at or below these frequencies can be used to probe nonlinear coefficients of lattice oscillator potentials. Measurements in the immediate neighborhood of the lattice resonance are necessary to determine mixed electronic-ionic terms.

A nonlinear phenomenon of a different kind recently discovered in our work[2] is a large $\chi^{(3)}$ contribution from free carriers in semiconductors. This nonlinearity becomes very strong in the far infrared, roughly where the frequency becomes of the order of the collision frequency. Theory and experiment on the free-carrier nonlinearity will be described separately in paper II, which will follow immediately.

In the present paper (I) we shall start (Sec. II) with the experimental procedures, common to I and II, of measuring far-infrared nonlinear coefficients by harmonic generation. The most significant step in the development of this experiment is the achievement of a new type of quasi-optical high-pass filter with high contrast, capable of selectively rejecting the fundamental radiation by many orders of magnitude.[3] Section III discusses the theoretical background of ionic frequency doubling, following Garrett's extension[4] of Miller's phenomenological concept,[5] by describing the electronic and ionic responses of an infrared-active crystal by two (anharmonically coupled) oscillators. The result is that nonlinear susceptibilities can be expressed as a function of the linear susceptibilities. While this model neglects local-field effects, these are definitely included in Flytzanis' quantum-mechanical microscopic derivation of the far-infrared nonlinear susceptibility of III-V compounds.[6]

Section IV describes and analyzes our experimental results on frequency doubling. Appendixes A and B supplement Sec. II by giving linear optical constants which we found necessary to measure in order to extract absolute nonlinear coefficients.

II. EXPERIMENTAL METHOD

Bulk nth harmonic generation ($n=2,3,\ldots$) is described by the well-known expression

$$P^{(n)}=\chi^{(n)}E^n ,$$

where E is the fundamental wave electric field, while $P^{(n)}$ and $\chi^{(n)}$ denote polarization and nonlinear susceptibility, respectively, of nth order.[7] The harmonic wave electric field is obtained by integrating Maxwell's equations with $P^{(n)}$ as the source term. In the simple case of plane waves traveling in the z direction with $\chi^{(n)}=0$ at $z<0$, and $\chi^{(n)}=\text{const}$ at $z \geq 0$, the solution is[8]

$$E_{n\omega}(z)=4\pi P^{(n)}(z=0)C(z) , \tag{1}$$

where

$$C(z)=\left[\exp\left[\frac{i\omega z}{c}(N_\omega - N_{n\omega})\right]-1\right]\Big/(N_\omega^2 - N_{n\omega}^2) . \tag{2}$$

Here, $N_u = n_u - ic\alpha(u)/2u$ is the complex refractive index

at frequency $u=\omega$ or $n\omega$, respectively. This formulation assumes a small-signal regime, i.e., the neglect of a depletion of the fundamental wave by the buildup of the harmonic wave.

Fortunately, phase matching does not present problems in the far infrared: As can be seen in Eq. (2), the oscillatory function, representing phase incoherence between fundamental and harmonic fields, has an argument which scales with the wavelength. Thus coherence lengths are quite large, typically of the order of absorption lengths. In many cases, harmonic conversion in the far infrared is therefore limited by absorption rather than by phase mismatch.

High intensity (1 MW/cm^2) is required to observe far-infrared harmonic generation. In order to avoid heating, we use single short pulses (40 ns), the substructure (1 ns) of which can still be fully resolved by standard oscilloscopes. The far-infrared laser consists of an 8-m-long mirrorless glass tube, 4 cm in diameter, with a gas fill of several Torr (Fig. 1). It is pumped with 5 J from a grating-tuned TEA-CO_2 laser (where TEA is the transversely excited atmospheric pressure). The far-infrared radiation is focused by f-4.5 optics to the harmonic crystal. This intensity suffices to obtain even dielectric breakdown in many materials. For harmonic spectroscopy covering one or two octaves of frequency, we found it convenient to use a single gas fill of 7-Torr CH_3F. This allows tuning the laser frequency from 20 to 57 cm^{-1} in 18 practically equidistant steps, while maintaining a pulse energy in excess of 1 mJ.[9]

Our experiment aims to absolutely determine $\chi^{(n)}$. Therefore we need to know $E_\omega(\mathbf{r},t)$ throughout the sample, preferably by using a single-mode beam. As for spatial structure, both the pump and, when properly aligned, the far-infrared beams, exhibit near-fundamental Gaussian mode profiles, $E\sim\exp(-r^2/w^2)$, where w is the spot radius [Fig. 1(a)].

There is, however, a very strong and irreproducible temporal structure [Fig. 1(b)] which stems from mode-locking effects in the CO_2 laser. We resorted to routinely measuring the far-infrared pulse shape using a photon-drag detector (resolution 0.6 ns) and processing it with an on-line computer [see Eq. (6) below]. The sample crystals used are thin enough to allow an approximation of the fields by plane waves. Slight wedge angles were used between input and exit surfaces to avoid standing-wave effects.

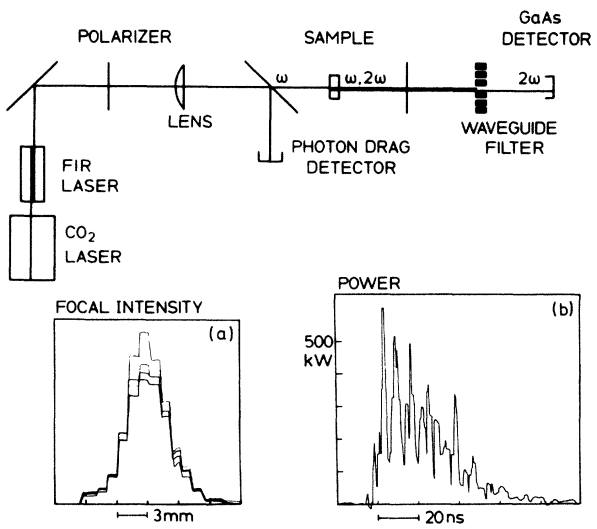

FIG. 1. Outline of far-infrared harmonic generation experiment. The insets show typical far-infrared mode profiles at the sample location. (a) Cross-sectional intensity distribution (six shots superimposed); (b) temporal structure of pulse power.

We can now state the field amplitudes outside the crystal

$$E_u^a=E_u(N_u+1)/2 \tag{3}$$

and find for the harmonic field leaving the crystal of length d

$$E_{n\omega}^a=4\pi\chi^{(n)}[E_\omega^a(z=0)]^n\frac{2^{n-1}(N_{n\omega}+1)}{(N_\omega+1)^n}C(d)\ . \tag{4}$$

Using the relation between intensity I and field amplitude, $I=cE^2/8\pi$, we obtain for the generated harmonic power,

$$L_{n\omega}(t)=(4\pi)^2\left[\frac{8\pi}{c}\right]^{n-1}\left|\frac{2^{n-1}(N_{n\omega}+1)}{(N_\omega+1)^n}\right|^2|\chi^{(n)}|^2[L_\omega(t)]^n\left[\frac{2}{\pi w^2}\right]^n\int|C(d)|^2\exp(-2nr^2/w^2)dF\ , \tag{5}$$

where $L_\omega(t)$ is the power of the fundamental wave incident on the sample.

In our experiment, we use a sensitive photoconductive GaAs detector to measure the harmonic radiation. Since its response is too slow to fully resolve $L_{n\omega}(t)$, we use it as a detector of harmonic pulse energy

$$W_{n\omega}=\int L_{n\omega}(t)dt\sim\int[L_\omega(t)]^n dt\ . \tag{6}$$

The latter integral is routinely obtained from the photon-drag detector signal as described above. For detector calibration, we use a pyroelectric energy meter (Laser Precision RYP 735 RF) which, however, has to be corrected for strong internal standing wave resonances in the far infrared (see Appendix B). As a result, we find that at the peak of its spectral response (35 cm^{-1}), the GaAs detector is capable of a minimal detectable pulse energy $W=5\times10^{-16}$ J.

Wire-grid linear polarizers are used to select the polarization of both the input and the harmonic waves. Separating off the fundamental from the harmonic radiation is done by a filter specifically developed for this work.[3] It consists of a perforated metal foil where the holes act as cut-off waveguides. These filters can be made to transmit well (up to 90%) in a relatively broad frequency range 0.9 f–1.1f but to transmit less than 10^{-9} for any frequency below 0.7 f. Table I lists the characteristics of the filters used.

TABLE I. Characteristics of metal waveguide filters used in this study. t, thickness of brass plate; d', diameter of drill; d, maximum diameter of drilled hole; g, period of square array of holes. A Fourier spectrometer was employed to measure the maximum transmission T_{max} and the lower frequency limit $\nu_{1/2}$, defined by $T(\nu_{1/2})=T_{max}$, of the high-transmission region. An upper frequency limit of the strongly rejected region, defined by $T(\nu_{10^{-9}})=10^{-9}$, is calculated from the waveguide data t and d (see Ref. 3).

d' (μm)	d (μm)	t (μm)	g (μm)	T_{max} (%)	$\nu_{1/2}$ (cm^{-1})	$\nu_{10^{-9}}$ (cm^{-1})
180	194	1030	400	3.7	32	25.7
150	170	1030	200	66	39	30.6
130	145	700	200	39	40	32.9
90	95	320	120	35	65	34.0
70	84	320	90	15	86	57.2

It is finally necessary to absolutely calibrate the response of the receiver consisting of the 3×3 mm^2 GaAs detector, mounted at the end of a 17° condensing cone in a cryostat, with the metal waveguide filter mounted on the outside of the quartz cryostat window. We performed this for each experiment by replacing the harmonic crystal with a calibrated, high-loss attenuator, and by changing the CO_2 laser's wavelength in order to generate a far-infrared frequency in the vicinity of the harmonic frequency (a remaining frequency mismatch of ~1 cm^{-1} is sufficiently small that differences in diffraction can be neglected). For attenuators we fabricated a series of plates of precisely known thicknesses of borosilicate glass "Tempax," the refractive index and absorption spectrum of which was precisely established (Appendix A).

III. THEORETICAL BACKGROUND

In this paper we deal with second-harmonic generation. This section describes models of the pertaining nonlinear susceptibility.

We start by quoting Miller's rule, which relates nonlinear susceptibilities to linear susceptibilities, roughly in the form $\chi^{(n)}(\omega_1,\ldots,\omega_n)\sim\chi^{(1)}(\omega_1)\times\cdots\times\chi^{(1)}(\omega_n)$.[5] This rule is derived by considering the anharmonic perturbation of an electronic oscillator. This formulation has been extended to include an additional ionic oscillator by Garret,[4] who found that the nonlinear susceptibility can be expressed as a function of linear susceptibilities, in the general form

$$\chi^{(2)}_{jkl}(\omega_3,\omega_2,\omega_1)=\sum_{abc}\delta^{abc}_{jkl}\chi^a_j(\omega_3)\chi^b_k(\omega_2)\chi^c_l(\omega_1)\ . \tag{7}$$

Here, χ^a_j denotes the linear susceptibility of oscillator a (electronic or ionic) for the electric field direction along the axis j. δ^{abc}_{jkl} are the generalized Miller coefficients, where the symmetry conditions hold $\delta^{abc}_{jkl}=\delta^{acb}_{jlk}=\cdots$. Although Eq. (7) is phenomenological and, in addition, does not take into account local-field effects, it has been successfully used to fit experimentally-determined nonlinear susceptibilities. For the important case of III-V compounds, the symmetry condition $\delta^{abc}_{jkl}=\delta^{acb}_{jkl}=\delta^{cab}_{jkl}=\cdots$ holds, and Eq. (7) can be brought into the simple form

$$\chi^{(2)}_{jkl}(\omega_3,\omega_2,\omega_1)=\chi^{(2)}_E\left[1+C_1\left[\frac{1}{D(\omega_1)}+\frac{1}{D(\omega_2)}+\frac{1}{D(\omega_3)}\right]+C_2\left[\frac{1}{D(\omega_1)D(\omega_2)}+\frac{1}{D(\omega_1)D(\omega_3)}+\frac{1}{D(\omega_2)D(\omega_3)}\right]+C_3\frac{1}{D(\omega_1)D(\omega_2)D(\omega_3)}\right], \tag{8}$$

where

$$D(\omega_n)=1-(\omega_n/\omega_t)^2+i\omega_n\gamma/\omega_t^2\ .$$

$\chi^{(2)}_E$ is the purely electronic second-order nonlinear susceptibility, ω_t is the frequency of the transverse optical phonon, and γ is the damping constant. Equation (8) was derived using a microscopic model by Flytzanis,[6] which does include local-field effects. Flytzanis has furthermore calculated the constants C_1, C_2, and C_3 using a quantum-mechanical model.

The constants $\chi^{(2)}_E$, C_1, C_2, and C_3 can be determined by a series of experiments. Frequency doubling with $\omega\gg\omega_t$ allows one to directly determine

$$\chi^{(2)}_E=\chi^{(2)}_{jkl}(2\omega,\omega,\omega)\ . \tag{9}$$

C_1 can then be obtained by measuring the electro-optic coefficient

$$\chi^{(2)}_{jkl}(\omega,\omega,0)=\chi^{(2)}_E(1+\chi^{(2)}_E C_1(1+C_1))\ . \tag{10}$$

Faust and Henry[10] have generalized this experiment by mixing the radiation of far-infrared lasers $\omega_{FIR}\approx\omega_t$ with visible radiation $\omega\gg\omega_t$. They were thus able to measure $\chi^{(2)}_{jkl}(\omega\pm\omega_{FIR},\omega,\pm\omega_{FIR})$.

When all frequencies involved are below ω_t, no term can be dropped in Eq. (8). Boyd *et al.*[1] performed measurements for this most general case, for a series of crys-

tals, by low-frequency modulation of microwaves at 1.9 cm^{-1}, i.e., far below ω_t. With the sole exception of an experiment with Te at 357 cm^{-1},[11] there is no measurement of second-order nonlinear susceptibilities in the frequency region 1.9 to 1000 cm^{-1}. In this work we report the measurement of second order nonlinear susceptibilities, in GaAs and $LiNbO_3$, in the range 20 to 57 cm^{-1}, which is below, but not too far from, the lattice resonance.

In order to determine the final two constants, C_2 and C_3, of Eq. (8), it is necessary to conduct an additional experiment, involving, e.g., the first three terms of Eq. (8), as, for example, frequency doubling across the lattice resonance, $\omega < \omega_t < 2\omega$. This separation of C_2 and C_3 would be interesting for distinguishing between two fundamental processes contributing to multiphonon lattice absorption.[12] Such an extension of our experiment is, however, difficult. Both the penetration and coherence lengths become very short because of strong absorption and dispersion, respectively, in the immediate neighborhood of the lattice resonance. It is unlikely that an absolute measurement of $\chi^{(2)}$ could succeed with the required accuracy. Therefore we propose an alternative way to experimentally separate C_2 and C_3 by a null method using a tunable laser, as will be discussed in Sec. IV, in connection with Fig. 3.

IV. EXPERIMENTAL RESULTS AND DISCUSSION

Absolute nonlinear susceptibilities were measured using wedge-samples. This geometry allows one to avoid Fabry-Perot effects and to conveniently determine coherence lengths, since by a simple translation, the sample thickness can be continuously varied.

A. GaAs

In the case of GaAs we used two single-crystal wedges with angles of 5° and 12°, and a maximum thickness of 1.2 cm. The surfaces were polished. With the orientation as shown in Fig. 2(a), the effective nonlinear susceptibility is $\chi_{\text{eff}}=(2/\sqrt{3})\chi_{14}$, where χ_{14} denotes the only independent component of the relevant nonlinear susceptibility tensor in symmetry class $\bar{4}3m$. Figure 2(b) shows the harmonic pulse energy leaving the sample, normalized to a mean value of $\int [L_\omega(t)]^2 dt$, with a mean incident fundamental pulse energy of 1.1 mJ [cf. Eq. (6)]. The shot-to-shot fluctuations are due to fluctuations of the mode radius w. The oscillatory behavior of $W_{2\omega}$, known as "Maker fringes," is due to dephasing between fundamental and harmonic waves. The damping of these oscillations is due to lattice absorption. The solid line in Fig. 2(b) is a theoretical fit using Eq. (4). The only fit parameter, $\chi^{(2)}$, is thereby determined. The linear refractive index entering in this procedure is calculated from an oscillator model

$$\epsilon=\epsilon_0+\Delta\epsilon\left[\frac{\omega_T^2}{\omega_T^2-\omega^2+i\gamma\omega}-1\right], \tag{11}$$

where

$$\epsilon=\left[n-\frac{ic\alpha}{2\omega}\right]^2 \tag{12}$$

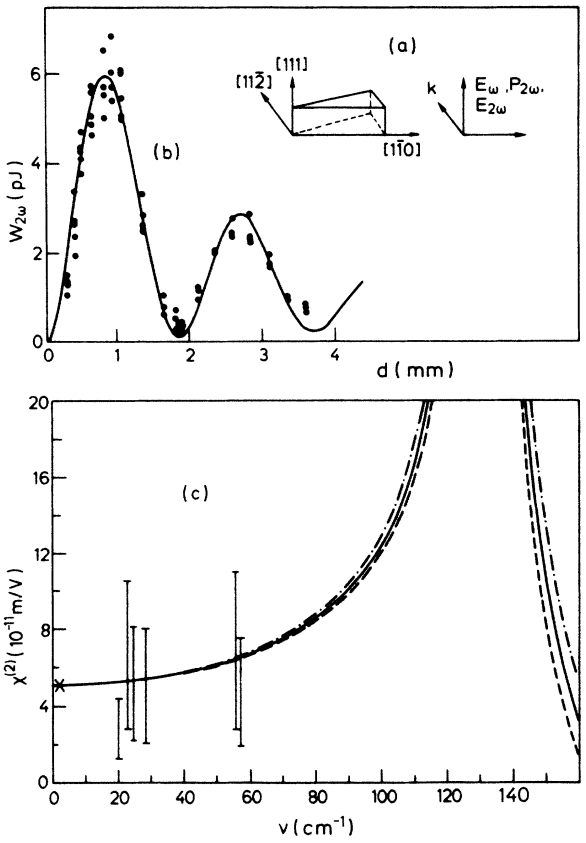

FIG. 2. Results of frequency-doubling experiments in GaAs. (a) Orientation of wedge-shaped sample, and polarization of fundamental and harmonic fields. (b) Harmonic pulse energy vs sample thickness at 56.8-cm^{-1} fundamental frequency, data points from single shots. The curve is a fit to Eq. (4). (c) Absolute nonlinear coefficient $\chi^{(2)}$ as derived from experiments at six frequencies. Data point at 1.9 cm^{-1} from Ref. 1. The curves result from theory (see text).

is the dielectric constant, ϵ_0 the static dielectric constant, and $\Delta\epsilon$ is the oscillator strength; ω_T is the radian frequency and γ is the damping parameter of the lattice resonance. We adopted the following values:[13] $\epsilon_0=13.5$, $\Delta\epsilon=1.95$, $\omega_T/2\pi=268.2$ cm^{-1}, $\gamma/2\pi=1.88$ cm^{-1}. This model is not sufficient to also calculate the absorption constant, because of an additional strong multiphonon absorption. Therefore, we determined α directly by transmission measurements (see Appendix A). The choice of the linear constants can be readily cross-checked from the nonlinear results [Fig. 2(b)]: The position of the first Maker minimum essentially gives $n_{2\omega}-n_\omega$, and the energy ratio of first- and second-Maker maximum is determined by absorption.

The experimental procedure of absolute measurement was performed at six far-infrared frequencies. The resulting absolute value of $\chi_{14}^{(2)}$ is shown in Fig. 2(c). The accuracy (error bars) is limited mainly by the absolute calibration of the harmonic energy measurement. Our data are thus in accordance with the microwave result[1] and do not show a frequency dependence. (The nonlinear susceptibility is given in MKS units as defined in Ref. 14. The con-

TABLE II. Experimental and theoretical constants entering the nonlinear susceptibility model Eq. (8) of GaAs.

	$\chi_E^{(2)}$ (10^{-12} m/V)	C_1	C_2	C_3	$3C_2+C_3$	$C_3/(3C_2)$
Experiment	134[a]	−0.59[b]			0.39[b]	
Theory[c]		−0.83	0.14	−0.07	0.35	−0.17

[a]Reference 18.
[b]Reference 6 and references therein.
[c]Reference 6.

version to cgs units as used in Secs. II and III is $\chi^{(2)}_{MKS}=10^{-4}4\pi/3\chi^{(2)}_{cgs}$.) Equation (8) is used to calculate the theoretical curves in Fig. 2(c). For three of the required constants, $\chi_E^{(2)}$, C_1, and $3C_2+C_3$, we can use experimental constants (Table II). For a fourth constant $C_3/(3C_2)$, which has yet not been experimentally determined, we use the theoretical value -0.17,[6] to obtain the solid curve in Fig. 2(c). In addition, we arbitrarily designate this value -0.10 and -0.23, to obtain the dashed and dashed-dotted curves, respectively, in Fig. 2(c). This choice is suggested by the order of disagreement, $\lesssim 40\%$, between theoretical and experimental values of C_1 and $3C_2+C_3$ (Table II). Clearly, the effect is very weak in the frequency range covered by our experiment. However, an extension of the calculations (Fig. 3) shows that frequency-doubling experiments at frequencies in the immediate neighborhood of the lattice resonance could well determine the unknown constant $C_3/(3C_2)$. The following two possibilities exist.

(a) As suggested previously[4,6] the nonlinear susceptibility could be absolutely determined, for a fundamental frequency near 225 cm^{-1}. Low temperature would be necessary to suppress multiphonon absorption. With 8-K oscillator data[15] we expect $\alpha_\omega=5.2$ cm^{-1}, $\alpha_{2\omega}=25.1$ cm^{-1}, $n_\omega=3.806$, $n_{2\omega}=2.865$, and thus a coherence length of 11.8 μm. Given a laser with pulse energy 1 mJ, pulse length 10 ns, and mode diameter 1 mm, a harmonic energy of 10^{-11} J can be expected, which can be detected with a Si bolometer. A KCl reststrahlen-filter can be used to separate the harmonic from the fundamental radiation. It may, however, be difficult to achieve the necessary absolute accuracy to within a factor of 2.

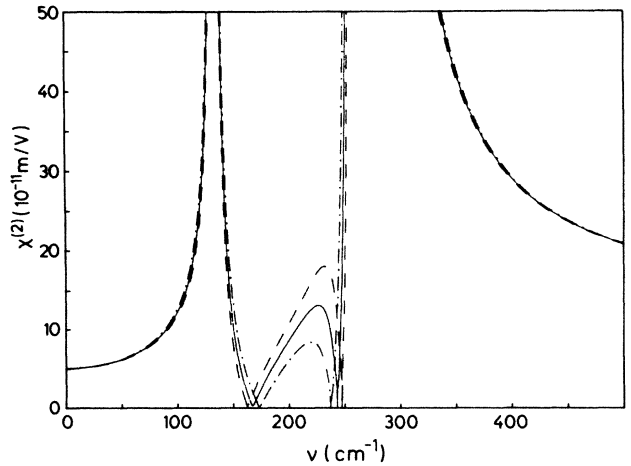

FIG. 3. Extension of theoretical nonlinear susceptibility [Fig. 2(c)] through the Reststrahlen region of GaAs. $\chi^{(2)}$ becomes negative between 165 and 245 cm^{-1}.

(b) Alternatively, we propose a more elegant procedure which avoids the crux of absolute energy calibration: By tuning the laser frequency, one could use frequency-doubling to find the frequency where $\chi^{(2)}$ changes sign and $W_{2\omega}$ becomes zero. Sensitive detectors could be employed to achieve high accuracy. Detector nonlinearity as it occurs, e.g., in the case of a superconducting bolometer, would not be of much disadvantage. This experiment would be possible with a tunable source such as the free-electron mid-infrared laser.

B. $LiTaO_3$

As a second material, we chose $LiTaO_3$, because its lattice resonance frequency is lower and thus nearer to the frequency region accessible in our present experiment. A single domain crystal wedge was prepared. An apex angle of only 1° was chosen because of the strong absorption. With the orientation used [Fig. 4(a)] the fundamental field is perpendicular to the [100] optical axis, while the har-

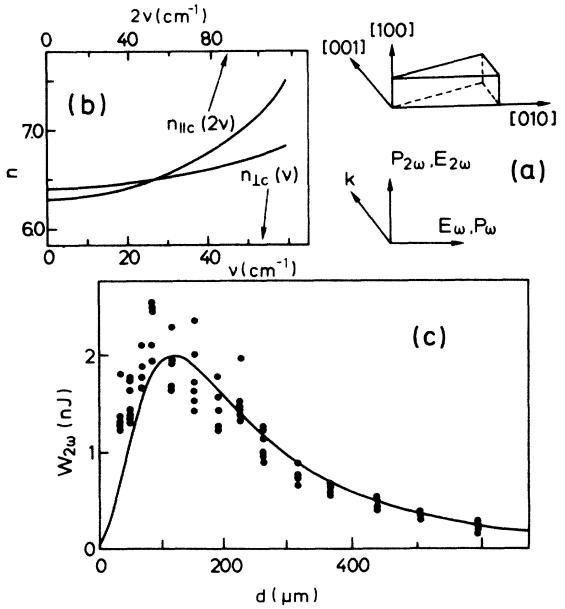

FIG. 4. Results of frequency-doubling experiments in $LiTaO_3$. (a) Orientation of sample and fields. (b) Dispersion of fundamental and harmonic waves. (c) Harmonic pulse energy vs sample thickness at 38.2-cm^{-1} fundamental frequency, data points from single shots. The curve is a fit to Eq. (4).

monic field is parallel. The nonlinear susceptibility effective in this geometry is $\chi_{\text{eff}}=\chi_{31}$, which is one out of four independent nonzero tensor components for the symmetry class $3m$. The linear refractive indices for both polarizations are shown in Fig. 4(b), as calculated from Eqs. (11) and (12) using[16]: $\epsilon_0=41.1$, $\Delta\epsilon=24.1$, $\omega_T/2\pi=142$ cm^{-1}, $\gamma/2\pi=14$ cm^{-1} for $\mathbf{E}\perp\mathbf{c}$; and $\epsilon_0=39.8$, $\Delta\epsilon=30.0$, $\omega_T/2\pi=200$ cm^{-1}, $\gamma/2\pi=28$ cm^{-1} for $\mathbf{E}\|\mathbf{c}$. Thus phase matching occurs at a fundamental frequency of 28 cm^{-1}. The absorption was determined by separate transmission experiments (Appendix B). Figure 4(c) shows an example of the nonlinear data obtained. Higher order Maker fringes are damped out by absorption over the relatively large coherence length.

We opted to determine the nonlinear susceptibility $\chi^{(2)}$ of $LiTaO_3$ not as an absolute quantity, but, rather, relative to the one of GaAs. In the experiment, $LiTaO_3$ and GaAs samples were alternatively exposed. The advantage is that the result is not affected by absolute detector calibration nor by fluctuations of the laser mode structure. This makes the determination of $\chi^{(2)}$ three times more accurate.

Ideally, a reference material should have no dispersion in the linear or nonlinear susceptibilities. GaAs is quite acceptable, since, up to a thickness of 0.5 mm, the influences of absorption and coherence lengths are small. The calculated nonlinear susceptibility shows only small dispersion, and it is furthermore not dependent on the unknown constant $C_3/3C_2$. Results of the relative measurements are shown in Fig. 5. The accuracy is now limited by the accuracy of the relative energy measurement and by the accuracy of determining the linear optical data of $LiTaO_3$. For $\omega\to 0$, our data agree with the microwave result of Boyd *et al.*[1] When the frequency approaches the reststrahlen region, the nonlinear susceptibility shows resonant enhancement.

For a comparison with theory we can apply Eq. (7) to write the appropriate tensor component ($\chi_{311}=\chi_{31}$):

$$\chi_{311}=\delta_{311}^{eee}\chi_3^e(2\omega)\chi_1^e(\omega)\chi_1^e(\omega)+2\delta_{311}^{eei}\chi_3^e(2\omega)\chi_1^e(\omega)\chi_1^i(\omega)+\delta_{311}^{iee}\chi_3^i(2\omega)\chi_1^e(\omega)\chi_1^e(\omega)$$
$$+\delta_{311}^{eii}\chi_3^e(2\omega)\chi_1^i(\omega)\chi_1^i(\omega)+2\delta_{311}^{iei}\chi_3^i(2\omega)\chi_1^e(\omega)\chi_1^i(\omega)+\delta_{311}^{iii}\chi_3^i(2\omega)\chi_1^i(\omega)\chi_1^i(\omega)\ . \tag{13}$$

The first three δ's of Eq. (13) are experimentally known (frequency-doubling far above the lattice resonance, electro-optic effect). The last three δ's can, in principle, be determined from the dispersion of the nonlinear susceptibility within and below the lattice resonance. For this purpose a wider frequency range is required than is available in our present experiment. In this situation it is helpful to notice the relatively strong *ionic* linear susceptibility of $LiTaO_3$, $\chi^i\approx 10\chi^e$. Assuming that the δ's have comparable magnitude, as stated by Miller's rule[5] for δ_{jkl}^{eee} [see Table I of Ref. 1(a) for ionic terms], $\delta_{311}^{iii}\approx\delta_{311}^{iei}\approx\delta_{311}^{eii}$, it suffices to retain the last term of Eq. (13),

$$\chi_{311}(2\omega,\omega,\omega)=\delta_{311}^{iii}\chi_3^i(2\omega)\chi_1^i(\omega)\chi_1^i(\omega)\ . \tag{14}$$

This equation describes the nonlinear susceptibility of a single anharmonic oscillator. Indeed, it fits our experimental data quite well (the curve in Fig. 5 is plotted with due account taken of the slight dispersion of the reference material, GaAs). The fit gives $|\delta_{311}^{iii}|=8\times 10^{-14}$ m/V.

From this value we can deduce quite directly the coefficient of the anharmonic lattice potential A_{311}^{iii}, using[1]

$$\delta_{311}^{iii}=-\tfrac{3}{2}\epsilon_0^2\frac{A_{311}^{iii}}{(n^i)^2(q^i)^3}\ , \tag{15}$$

where ϵ_0 in this formula is the dielectric permittivity of vacuum, and n^i and q^i are the density and charge, respectively, of the ionic oscillator. With the values

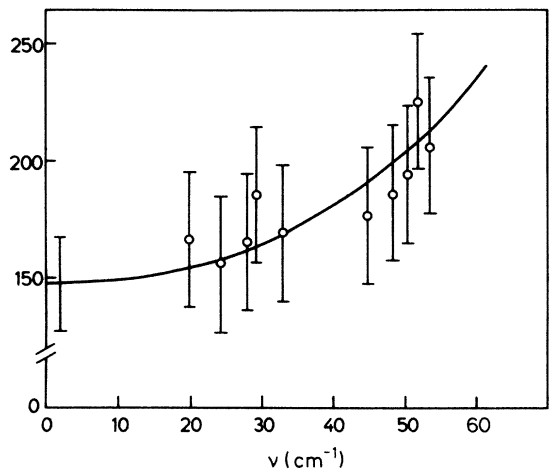

FIG. 5. Nonlinear susceptibility of $LiTaO_3$, normalized to GaAs as $\chi_{31}^{(2)}(2\omega,\omega,\omega;\ LiTaO_3)/\chi_{14}^{(2)}(2\omega,\omega,\omega;\text{GaAs})$ vs fundamental frequency. Data point at 1.9 cm^{-1} from Ref. 1. The curve results from a fit to an ionic oscillator model.

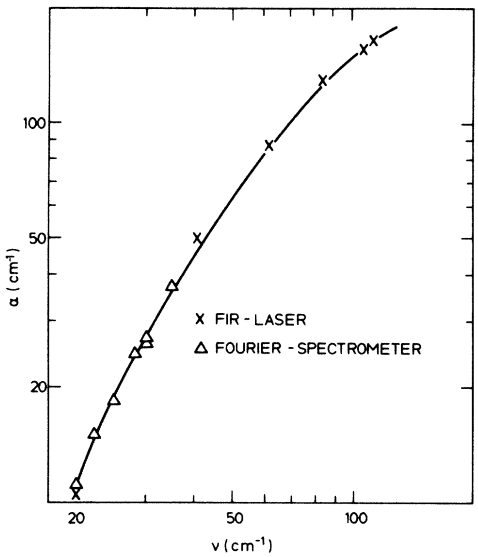

FIG. 6. Absorption coefficient of borosilicate glass "Tempax" (Schott type 3.3), vs frequency.

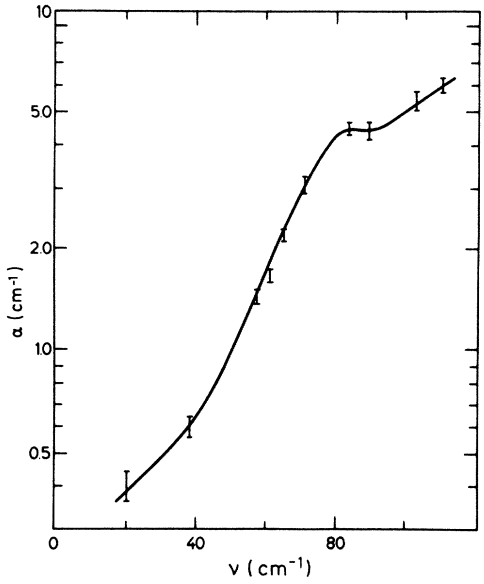

FIG. 7. Absorption coefficient of GaAs, vs frequency.

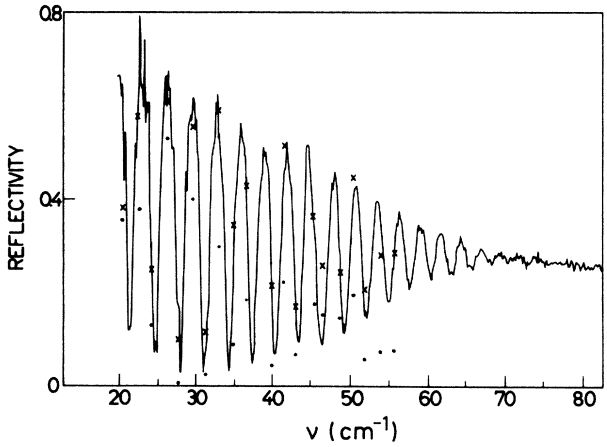

FIG. 9. Reflectivity spectrum of pyroelectric detector (Laser Precision RYP 735 RF). The data points are from laser measurements; solid circles and crosses denote p- and s-polarized incidence, respectively, on the detector crystal. The uncalibrated Fourier spectrum (solid curve) has been adjusted in height to overlap the s-polarized laser points.

$n^i = 1.9\times10^{28}$ m^{-3}, $q^i = 1.3\times10^{-18}$ C^1 we deduce the anharmonic coefficient to be $|A^{iii}_{311}| = 8\times10^{11}$ J/m^3.

V. CONCLUSIONS

We have developed a technique to determine absolute nonlinear susceptibilities for bulk second-harmonic generation in the far infrared. GaAs and $LiTaO_3$ were studied in detail, while second-harmonic response was readily observed in many other crystals, e.g., GaP, ZnO, $LiNbO_3$, and $LiTo_3$. These measurements can be used to determine anharmonic terms of lattice oscillator potentials. An extension of the experiments toward higher frequencies, using, e.g., free-electron-lasers, seems highly desirable.

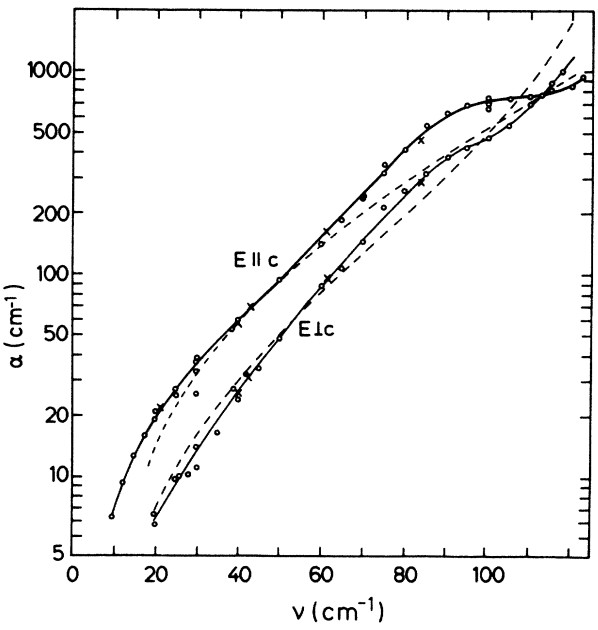

FIG. 8. Absorption coefficient of $LiTaO_3$ vs frequency, with the electric field parallel or perpendicular to the optical axis. The experimental data are from a Fourier spectrometer (circles) and a laser system (crosses). They are connected by the solid curve. The dashed curves represent an oscillator model.

APPENDIX A

The far-infrared linear optical constants of GaAs, $LiTaO_3$, and borosilicate glass "Tempax" (Schott type 3.3) were determined. A series of samples with several thicknesses was prepared. The measurements were taken, at room temperature, with a Fourier spectrometer and a c.w. far-infrared gas laser. The latter has the advantage of high power and is usable with samples of low transmission. The Fourier spectrometer is used with samples of high transmission; it has the advantage of large frequency coverage allowing refractive index measurements through Fabry-Perot effects. Figure 6 shows the absorption of borosilicate glass which we used for calibrated attenuation.

Figure 7 shows the absorption of GaAs, which agrees well with earlier data.[17] Figure 8 shows the absorption of $LiTaO_3$ for both polarizations. The experimental data are compared to an oscillator model, after Eq. (11), using $\omega_T = 142$ cm^{-1} and $\gamma = 14$ cm^{-1}, for E⊥c.[18] For E∥c we use $\gamma = 45^{-1}$ cm^{-1}, whereas Barker *et al.*[16] obtain $\gamma = 28$ cm^{-1} from reflection measurements. Multiphonon absorption could account for this discrepancy. The absorption coefficients which are used by Barker *et al.* to fit their absorption data,[16] $\gamma = 50$ cm^{-1} for E⊥c, and $\gamma = 84$ cm^{-1} for E∥c, give absorption coefficients which are far too large.

APPENDIX B

A pyroelectric energy meter (Laser Precision RYP 735 RF) is employed to absolutely determine the laser pulse

energy. This detector is, however, specified to fully absorb in the visible to mid-infrared regions only. To extend the calibration into the far infrared, we assume that incident radiation is either absorbed or reflected from the detector. Hence a measurement of the reflectivity can serve to give the appropriate correction. The detector crystal comes mounted in a circular metal tube of 1 cm inner diameter. The crystal surface is inclined about 30° in respect to the tube axis, filling the whole aperture. This geometry causes difficulty for a reflection measurement, since the reflected radiation is angularly dispersed.

The reflectivity spectrum taken with a Fourier spectrometer thus contains an unknown calibration factor. However, we found that with using our laser and a short focal length lens, all of the reflected radiation can be collected and detected on a second detector, thus allowing absolute calibration against a plane metal mirror used as reference. The resulting spectrum (Fig. 9) can be interpreted to arise from standing wave resonances in the detector crystal which die out at higher frequencies where, owing to increased absorption, only the first surface reflectivity is seen.

ACKNOWLEDGMENTS

We gratefully acknowledge the help of D. Mead and E. J. Danielewicz in the initial phase of this work, as well as the contribution of K. W. Kussmaul of fabricating the waveguide filters. We thank C. Flytzanis for bringing Refs. 6 and 11 to our attention.

---

*Present address: Prognos AG, Steinengraben 42, 4011 Basel, Switzerland.

[1](a) G. D. Boyd, T. J. Bridges, M. A. Pollack, and E. H. Turner, Phys. Rev. Lett. **26**, 387 (1971); (b) M. A. Pollack and E. H. Turner, Phys. Rev. B **4**, 4578 (1971); (c) G. D. Boyd and M. A. Pollack, Phys. Rev. B **7**, 5345 (1973).

[2]A. Mayer, Ph.D. thesis, University of Stuttgart, 1984.

[3]F. Keilmann, Int. J. Infrared Millimeter Waves **2**, 259 (1981).

[4]C. G. B. Garrett, IEEE J. Quantum Electron. QE-4, 70 (1968).

[5]R. C. Miller, Appl. Phys. Lett. **5**, 17 (1964).

[6]C. Flytzanis, Phys. Rev. B **6**, 1264 (1972).

[7]N. Bloembergen, *Nonlinear Optics* (Benjamin, New York, 1965).

[8]N. Bloembergen and P. S. Pershan, Phys. Rev. **128**, 606 (1962).

[9]C. T. Gross, J. Kiess, A. Mayer, and F. Keilmann, IEEE J. Quantum Electron. (to be published).

[10]W. L. Faust and C. H. Henry, Phys. Rev. Lett. **17**, 1265 (1966).

[11]G. H. Sherman and P. D. Coleman, J. Appl. Phys. **44**, 238 (1973).

[12]C. Flytzanis, Phys. Rev. Lett. **29**, 772 (1972).

[13]S. Iwasa, I. Balslev, and E. Burstein, in *Proceedings of the International Conference on the Physics of Semiconductors,* edited by M. Hulin (Dunod Cie, Paris, 1964), p. 1077.

[14]R. Bechmann and S. K. Kurtz, in *Landolt-Börnstein, Zahlenwerte und Funktionen aus Naturwissenschaft und Technik,* Gruppe III: Kristall- und Festkörperforschung, Band 2, edited by K. H. Hellwege (Springer-Verlag, Berlin, 1969).

[15]C. J. Johnson, G. H. Sherman, and R. Weil, Appl. Opt. **8**, 1667 (1969).

[16]A. S. Barker, A. A. Ballmann, and J. A. Ditzenberger, Phys. Rev. B **2**, 4233 (1970).

[17]R. H. Stolen, Appl. Phys. Lett. **15**, 74 (1969).

[18]J. J. Wynne and N. Bloembergen, Phys. Rev. **188**, 1211 (1969); J. H. McFee, G. D. Boyd, and P. H. Schmidt, Appl. Phys. Lett. **17**, 57 (1970).